

# PRECISE AIRSPEED VECTOR DETERMINATION AT THE NOSE OF AN AIRCRAFT

M. Dieroff and D. Martens  
 Institute of Flight Guidance and Control  
 Braunschweig Technical University  
 Hans-Sommer-Str. 66  
 D-38106 Braunschweig, Germany

19th ICAS Congress/AIAA Aircraft Systems Conference, Anaheim, USA  
 September 18–23, 1994

## Abstract

The Institute of Flight Guidance and Control of the Braunschweig Technical University operates a twin engine Dornier 128-6 research aircraft. To determine the airflow angles and the dynamic pressure it is equipped with a five-hole-probe mounted on the tip of a 3.5 m nose boom. This classical method is applied to minimize airflow interferences caused by the fuselage, wings and engines. Thus, accurate air data measurements are obtained. But there are some disadvantages as the need to modify the aircraft's front structure, the boom's oscillations and the length of the pneumatic lines inside the boom.

The solution to these problems is found by using the nose of the aircraft itself as a flow angle sensor. For this, there are only a few modifications necessary at the nose cover. The calibration of this sensor is performed online and in-flight having the advantage that the aerodynamical effects caused by the fuselage, wings and engines are automatically taken into account.

## Introduction

The knowledge of the angles of airflow is necessary for a number of research areas as e.g. aerodynamics and flight mechanics (determination of aircraft performances and flying qualities), flight control, design of gust alleviation systems or meteorology (calculation of wind and turbulence).

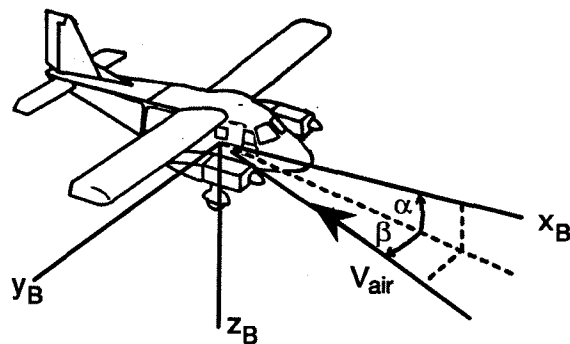


Figure 1: Definition of the angle of attack  $\alpha$  and the angle of sideslip  $\beta$

Especially this last discipline requires an accurate determination of the flow angles in a wide frequency range<sup>(3)</sup>.

The airspeed vector is generally defined by its absolute value and its direction. The direction is described by the angle of attack  $\alpha$  and the angle of sideslip  $\beta$  between the aircraft's longitudinal axis and the airflow vector (see fig. 1).

At the Dornier 128-6 research aircraft operated by the Institute of Flight Guidance and Control of the Technical University of Braunschweig the airflow direction is measured with the help of a five-hole-probe located at the tip of a nose boom (see fig. 2). The principle of operation of this flow angle sensor is the sensing of differential pressures between ports positioned on a hemispherical head

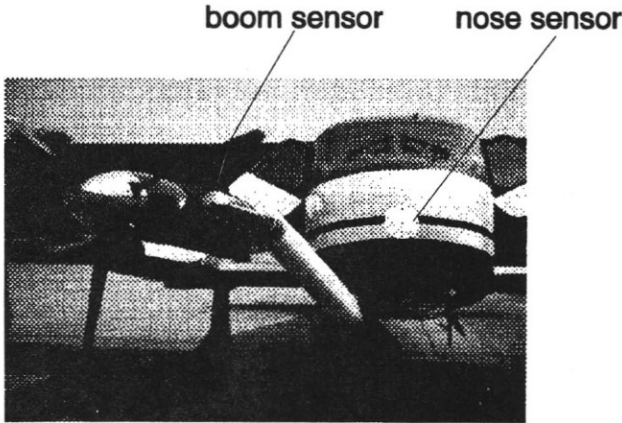


Figure 2: Dornier 128-6 research aircraft with nose boom and modified nose cover

as shown in fig. 3. When the aircraft flies at zero angle of attack the pressure difference between the ports is zero. As the aircraft rotates to higher angles of attack the pressure at the lower port increases, thus, being this pressure differential a function of  $\alpha$ . The angle of sideslip is obtained in a similar manner by rotating the ports  $90^\circ$  around the longitudinal axis.

The long nose boom is used to minimize airflow interferences caused by the fuselage, wings and engines. Thus, accurate air data measurements are obtained. But there are two major disadvantages:

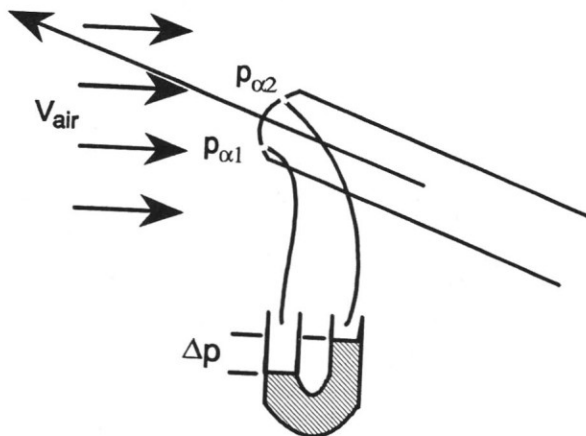


Figure 3: Principle of measurement for angle of attack

1. the eigenfrequencies of the boom influence the quality of the measurements
2. due to the lack of space inside the boom the pressure transducers cannot be mounted right behind the five-hole-probe which results in disturbing air oscillations inside the long pneumatic lines needed to transfer the pressure to the transducers.

The theoretical value of the eigenfrequency of the nose boom is of about  $14 \text{ Hz}$  and that of the air in the pneumatic transmission lines with a length of  $3.5 \text{ m}$  of about  $17 \text{ Hz}$ . These frequencies do not allow an accurate determination of the turbulence speed within these frequency ranges.

The following chapters describe an alternative method to measure the flow angles that allows for a more accurate determination of high dynamical angle changes. Concluding, some results obtained in flight tests are discussed.

#### Description of the technique

The principle of measurement applied in this method is the same as described above, but with the difference that the flow angle sensor is the nose of the aircraft itself. The pressure transducers are mounted behind the surface bores yielding a maximum length of only  $0.4 \text{ m}$  for the pneumatic transmission lines.

By using the nose as a flow angle sensor the nose boom oscillation is avoided and the shorter transmission lines allow for a frequency of approximately  $126 \text{ Hz}$  which is more suitable for accurate high frequency turbulence determination. An additional advantage of using the nose as a flow angle sensor is that the aircraft's front structure does not have to be strengthened to bear the nose boom.

To allow an accurate determination of the flow angles the nose cover of the fuselage has to be modified to get a hemispherical shape which is necessary to have a linear relation between the flow angles and the measured differential pressures. This relation is described by:

$$\alpha = k \cdot \Delta C_{p1,2} \quad (2.1)$$

$$\beta = k \cdot \Delta C_{p3,4} \quad (2.2)$$

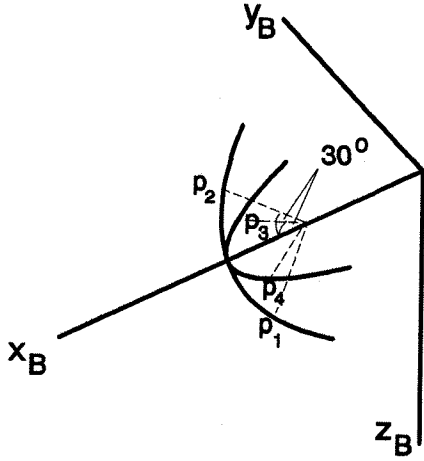


Figure 4: Location of the pressure ports at the nose of the aircraft

where

$$k = 14.7^\circ \quad (2.3)$$

is a sensitivity coefficient necessary to convert the dimensionless differential pressure coefficients into degrees. The value for  $k$  given above is valid only for low subsonic speeds and an aperture angle between the holes of  $30^\circ$  (see fig. 4). The differential pressure coefficients  $\Delta C_{p_{1,2}}$  and  $\Delta C_{p_{3,4}}$  are defined by

$$\Delta C_{p_{1,2}} = \frac{p_1 - p_2}{q_\infty} \quad (2.4)$$

$$\Delta C_{p_{3,4}} = \frac{p_3 - p_4}{q_\infty} \quad (2.5)$$

The dynamic pressure is the difference between the local pitot pressure and the local static pressure

$$q_\infty = p_t(V_{air}) - p_s(H) \quad (2.6)$$

$q_\infty$  is a normalizing function to account for the dependency of the pressure differentials  $\Delta p_{1,2}$  and  $\Delta p_{3,4}$  on airspeed and altitude.

### Calibration

The calibration of this new system is performed online and in-flight. During horizontal flight and calm air conditions the angle of attack  $\alpha$  may

be determined by measuring the pitch angle  $\Theta$ . This may be done e.g. by means of an inertial measuring unit (IMU). The angle of sideslip  $\beta$  is calibrated using the online calculation of the wind speed vector. With an inaccurate calibration the wind speed and wind direction changes correlate with changes of  $\beta$ . This kind of calibration takes all influences into account that occur around the real aircraft, which would be almost not possible in a wind tunnel.

The calibration of the  $\alpha$  sensor is performed at different airspeeds by adjusting different throttle positions in steps and at constant altitude. These steps range in the case of the Dornier 128-6 from approximately 70 *kts* to 150 *kts* of indicated airspeed. At each of these steps a different angle of attack is obtained. In general, the angle of attack is a function of pitch angle  $\Theta$ , flight path angle  $\gamma$  and wind angle  $\alpha_W$ :

$$\alpha = \Theta - \gamma + \alpha_W \quad (3.7)$$

During calm air conditions ( $\alpha_W = 0$ ) and horizontal flight ( $\gamma = 0$ ) the axes of airflow and flight path fall into the earth's horizontal plane. Thus, the pitch angle may be used as a reference for  $\alpha$ :

$$\alpha_{ref} = \Theta \quad (3.8)$$

By measuring the pitch angle a direct calculation of the calibration coefficients for the angle of attack is possible by linear regression:

$$\alpha_{ref} = \alpha_0 + \underbrace{k_F k}_{k_\alpha} \Delta C_{p_{1,2}} \quad (3.9)$$

The coefficients  $\alpha_0$  and  $k_\alpha$  denote offset and linear sensitivity of the angle of attack measurement respectively.  $k_F$  accounts for the corrections of the sensitivity coefficient due to the influence of the fuselage, wings and engines on the airflow and should be ideally approximately equal to one.

The in-flight calibration of the angle of sideslip is performed similarly. Different angles of sideslip are adjusted with rudder and aileron deflections at a constant airspeed.

In this case the angle of sideslip cannot be compared directly to the yaw angle  $\Psi$  because there is

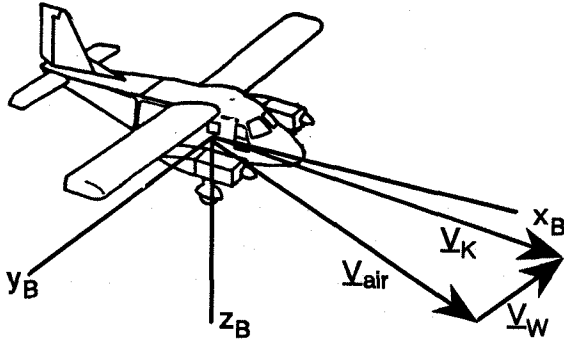


Figure 5: Determination of the wind speed vector

no usable natural reference in this plane. Therefore the institute applies an especially developed procedure that takes into account that an error in the  $\beta$  calibration produces an error in the calculation of the components of the horizontal wind. The vector of the wind speed itself is calculated by determining the difference between the flight path speed and the airspeed (fig. 5):

$$\underline{V}_W = \underline{V}_K - \underline{V}_{air} \quad (3.10)$$

$\underline{V}_K$  may be measured with an integrated navigation system (GNSS/IMU<sup>†</sup>). Accuracies of 10  $\frac{cm}{s}$  with such a system are state of the art. The relation between the  $\beta$  error and the horizontal wind speed error is described by the following equation<sup>(1)</sup>:

$$\Delta\beta = \frac{1}{V} \frac{\Delta u_{Wg} \sin \Psi + \Delta v_{Wg} \cos \Psi}{1 - 2 \cos^2 \Psi} \quad (3.11)$$

The reference signal for the angle of sideslip is the difference between the measured angle  $\beta_m$  and the above given error  $\Delta\beta$ . With eq. 3.11 only the sensitivity of the  $\beta$  signal may be calculated as the offset produces an error in the wind speed components as well. The offset may be calculated by determining the change of the wind speed components at eastbound and westbound flights<sup>(1)</sup>:

<sup>†</sup>GNSS: Global Satellite Navigation System, IMU: Inertial Measuring Unit

$$\Delta\beta_0 = \frac{u_{Wg,east} - u_{Wg,west}}{V(\sin \Psi_{east} - \sin \Psi_{west})} \quad (3.12)$$

Thus, the reference signal for the angle of sideslip is given by:

$$\beta_{ref} = \beta_m - \Delta\beta - \Delta\beta_0 \quad (3.13)$$

The calibration of the angle of sideslip is accomplished – analogously to the angle of attack – by determining the coefficients of the following linear function:

$$\beta_{ref} = \beta_0 + \underbrace{k_F k}_{k_\beta} \Delta C_{p3,4} \quad (3.14)$$

Here, again,  $k_F$  denotes a correction factor for the influence of the aircraft on the flow of air.

### Flight test results

The attachment of the boom of the research aircraft is located behind and below the cover that contains the pressure ports for the flow measurement at the nose. Thus, it has an offset to the aircraft's longitudinal axis  $x_B$  (see fig. 2) and the aircraft may be operated with both sensors simultaneously. This procedure allows an accurate comparison of both airflow sensors. As the research aircraft is not equipped with a fuselage mounted static sensor, the dynamic pressure is calculated by using the pitot and static pressures of the boom sensor.

The accuracy of any airflow sensor is deteriorated by several effects<sup>(2)</sup>. Among others there are to mention:

- inaccurate hemispherical shape of the sensor head,
- inaccurate positioning of the pressure ports,
- Reynolds-Number effects,
- Mach-Number effects, and, last but not least,
- airflow interferences due to fuselage, wings and engines.

	$\alpha_0$	$k_\alpha$	$\beta_0$	$k_\beta$
Boom	6.996°	12.12°	-0.39°	11.16°
Nose	0.850°	12.92°	0.0° <sup>†</sup>	14.70° <sup>†</sup>

Table 1: Calibration coefficients (†: theoretical values)

The calibration coefficients calculated in-flight are summarized in table 1. The calibration procedure takes into account all the effects described above. During flight tests the Dornier 128-6 is flown with angles of attack of about 7° at an indicated airspeed of 120 *kts*. In order to obtain accurate results the boom sensor  $\beta_0$  was designed to have exactly this offset to the longitudinal axis of the aircraft. This causes the value of  $\alpha_0$  of approximately 7°.

#### Stationary accuracy

Figs. 6 and 7 show the excellent conformity between the angles of attack and sideslip measured at the tip of the boom and at the nose of the aircraft. The angles of attack of both sensors deviate by only 0.5° at higher angles. It should be pointed out that the stall warning set into action at a speed of 80 *kts* ( $\alpha \approx 12^\circ$ ) which means that a steady horizontal flight could not be maintained satisfactorily at lower speeds.

In the case of higher angles of sideslip the absolute values for  $\beta_{boom}$  are up to 1.5° higher than those of  $\beta_{nose}$  (see fig. 7). The reason lies in the above described angle of attack of about 7° that is necessary to maintain a stationary horizontal flight at 120 *kts* during which the  $\beta$  measurements are performed. This unsymmetrical flow around the nose produces the pressure differential between the  $\beta$  ports to be smaller than they would be at  $\alpha = 0$ .

#### Dynamic accuracy

Frequency analyses show the expected improvement in the dynamics of the nose probe compared to that of the boom. Figs. 8 and 9 show the power density spectra of the angle of attack sensor at the tip of the boom and at the nose respectively. The sampling frequency of this data was of 50 *Hz*. Due to this rather low frequency the eigenfrequencies of the boom oscillation ( $f_1$ ) and

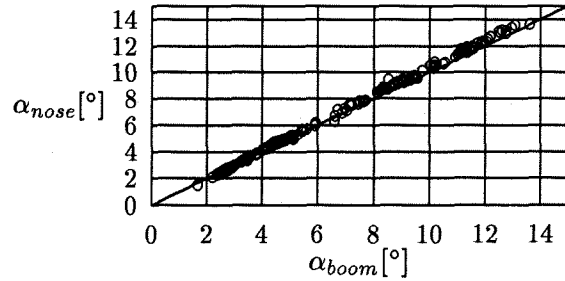


Figure 6: Comparison of the angle of attack measured at the boom to the angle of attack measured at the nose of the aircraft (test flight – March 30, 1994)

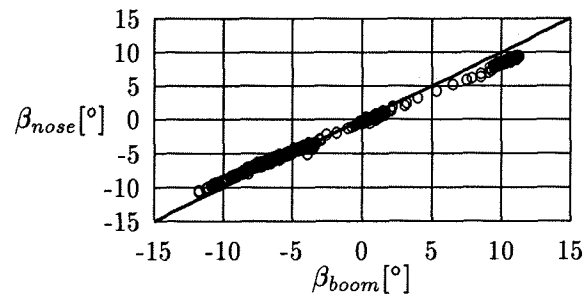


Figure 7: Comparison of the angle of sideslip measured at the boom to the angle of sideslip measured at the nose of the aircraft (test flight – March 30, 1994)

of the air in the transmission lines ( $f_2$ ) cannot be pointed out clearly but the peaks near these frequencies are still recognizable in fig. 8. In fig. 9 these peaks do not appear as no structural oscillation takes place and the air oscillation frequency is shifted to a higher value by using shorter transmission lines.

#### Concluding remarks

The fuselage, wings and engines of an aircraft considerably reduce the accuracy of flow angle measurements performed within the disturbed airflow if a calibration is applied that does not take these effects into account.

The development of the above described special in-flight calibration procedure allows a precise measurement of the airspeed vector at the nose of an aircraft. The simultaneous measurement of

the angles of airflow at the tip of a boom and at the nose of an especially equipped research aircraft demonstrated the feasibility of this method. It reduces costs and aircraft modifications significantly.

### Acknowledgement

This work has been supported by the 'Deutsche Forschungsgemeinschaft' within the special research area 'Sonderforschungsbereich 212'.

### References

- (1) *Vörsmann, P.:* An On-line Realization for Precise Wind Vector Measurements on Board the Do 28 Research Aircraft, ICAS-84-5.10.1, 14th ICAS Congress, Toulouse, 1984
- (2) *Wuest, W.:* Pressure and Flow Measurements, AGARD-AG-160-Vol. 11, 1980
- (3) *Jacobi, C.; Roth, R.:* Flugzeuggestützte Messungen meteorologischer Parameter an einer Kaltfront über der Nordsee, Meteorol. Z., 1, p. 195-206, 192

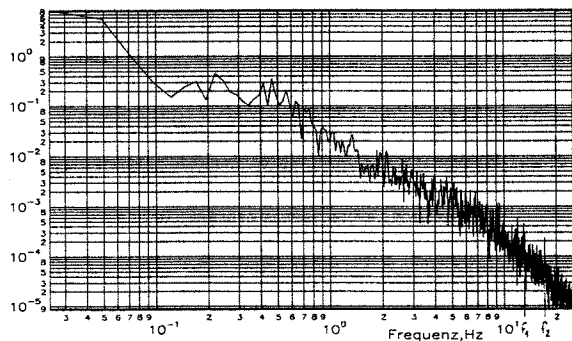


Figure 8: Power density spectrum of the angle of attack signal taken at the tip of the boom

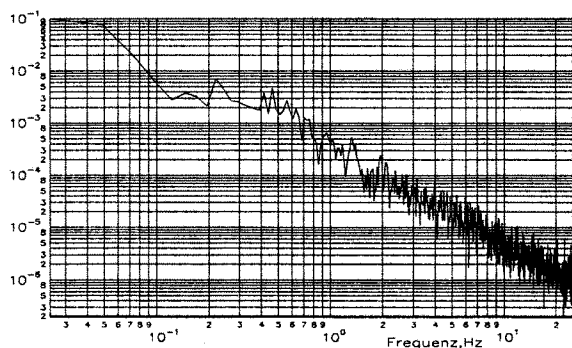


Figure 9: Power density spectrum of the angle of attack signal taken at the nose of the aircraft